LES simulations of enclosure fire scenarios with mechanical ventilation using EDC combustion model with finite-rate chemistry mechanisms

Jeri At Thabari[a*], Georgios Maragkos[a], Youk Moorthamers[a], Alexander Snegirev[a], Hugues Prétrel[b], Bart Merci[a]

[a]Department of Structural Engineering and Building Materials, Ghent University, Technologiepark 60, B-9052, Zwijnaarde, Belgium

[b]Autorité de Sûreté Nucléaire et de Radioprotection (ASNR), PSN-RES/SA2I/LEF, F-13115, Saint Paul lez Durance, France

*Corresponding author: jeri.atthabari@gmail.com

Abstract

Large-eddy simulations (LES) of fire in mechanically ventilated enclosures are conducted to evaluate the eddy dissipation concept (EDC) combustion model with finite-rate chemistry. Both well- and under-ventilated conditions are studied, with predictions compared to experimental measurements of temperature, heat release rate (HRR), and air supply. Three global mechanisms for propane are tested, alongside variations in fire size and ventilation flow rate. The results show limited grid sensitivity in the temperature predictions. For well-ventilated cases, the 2sWD mechanism yields less than 15% discrepancy above the burner, while the upper layer temperatures are generally underestimated due to over-predicted air supply. Good agreement of the predicted HRR is also observed, even on relatively coarse grid. The ventilation flow rates exert a stronger influence on the temperature predictions than the fire size. The prescribed boundary condition at the walls strongly influences the flow field and the flame appearance. Extinction in the under-ventilation scenario is captured, albeit with a delay of up to 100 s. An oscillatory behavior of the HRR in this scenario is observed. This could not be confirmed experimentally for safety reasons. Overall, the study highlights the critical role of flow–flame interactions and the need for quantitative flow-field measurements for further validation.

Keywords: CFD; enclosure fires; finite-rate chemistry; fire dynamics; EDC; well-and under-ventilated conditions

Highlights

- LES with the EDC finite-rate chemistry approach are validated in enclosure fire scenarios.
- 2sWD performs better in predicting the temperature and the HRR compared to other reaction mechanisms.
- The ventilation rate has a stronger impact on temperature results than the fire HRR.
- Boundary conditions at walls significantly influence the flow and flame shape.
- HRR oscillations and local extinction are observed for the under-ventilated scenario.

1. Introduction

The use of computational fluid dynamics (CFD) simulations in the fire engineering community is increasingly important. Practically, it serves as a reasonable way to provide complex physical analysis without spending as many resources as required for experiments. This aspect is significantly beneficial when the fire risk assessment needs to consider scenarios which are too demanding for experimentalists (i.e., big atria, high rise buildings, complex residential buildings, etc.). In order to have confidence in the output provided by the simulations, the numerical approaches/models need to be validated, and the common practice is to do this with reduced-scale experiments.

The most widely employed approach in CFD fire simulations relies on the assumption that combustion happens at a fast rate (mixing-controlled), neglecting the importance of chemistry in the combustion process. This approach is well known as a 'fast chemistry approach'. The two most famous models are the eddy dissipation model (EDM) [1] and the eddy dissipation concept (EDC) [2]. This approach is widely used due to its simplicity and relatively good accuracy when simulating free-burn [3] and in well-ventilated enclosure fire scenarios [4]. However, the primary disadvantage of these models is that they require additional sub-models for flame extinction, e.g., often based on a critical flame temperature [5] or a critical Damköhler number [6]. To avoid this, the combustion model should account for chemical kinetics through a 'finite-rate chemistry approach'. Although EDC has been initially developed for Reynolds-averaged Navier Stokes (RANS) models [7], it has also been extended to the large eddy simulations (LES) approach and has been previously tested for simulating open fire scenarios [8, 9] and extinction scenarios [10].

In enclosure fire scenarios, the flow field is determined by the fire-induced buoyancy as well as by the compartment boundaries and the (natural or mechanical) ventilation settings. In particular for mechanical ventilation, it is clear that the fire/flame is not the only driving force for the flow field. The higher the mechanical ventilation rate, the more dominant the induced flow field will become. Multiple flow rates are therefore considered in the present study. Nevertheless, in the absence of detailed flow field measurements, the focus will be on the impact of the turbulent combustion model in the simulation results. As such, this work is a continuation of authors' previous work on assessment of EDC in LES of fire simulations with the finite-rate chemistry approach. The focus is on the validation of the aforementioned approach in an enclosure fire scenario with mechanical ventilation.

To the best of the authors' knowledge, the validation of EDC with finite-rate chemistry in LES fire simulations is limited in such scenarios. A notable exception is [11], considering a backdraft phenomenon in an enclosure. The prediction highlights the accuracy of EDC with finite-rate chemistry in capturing the transient overpressure. Unfortunately, the model validation against the experiments was limited to this variable. As it stands, further validation of EDC with finite-rate chemistry approach in fire simulations is still much needed.

The study considers experiments performed by ASNR (Autorité de Sûreté Nucléaire et de Radioprotection, France) in a reduced-scale enclosure named 'NEXTC' [12, 13]. The available measurements from the experiments, such as thermocouple temperatures, HRR, and air supply flow rates, are compared with the CFD results. A sensitivity study is considered in the simulations by varying the ventilation flow rate, the fuel flow rate (i.e., fire size), and the

(global) chemistry mechanisms, on top of a sensitivity analysis on the grid size effect. Lastly, the effect of the boundary condition (BC) for velocity at the walls is also discussed.

2. Material and methods

2.1 Test case

The NEXTC configuration has been developed at ASNR, starting from the previous NYX set-up [13]. The enclosure (inner dimensions are 1.5 m (L) × 1.25 m (W) × 1 m (H) = 1.875 m³) consists of a metal frame, which allows modifications of the wall for specific purposes. For the tests considered here, the floor, side walls and ceiling are made up of a 23 mm layer of calcium silicate (ρ = 770 kg/m³, k = 0.185 W/K/m, c_p = 970 J/Kg/K) and a 3 mm steel sheet (ρ = 7817 kg/m³, k = 51.9 W/K/m, c_p = 446 J/Kg/K). One of the side walls (i.e., left wall, 1 m x 1.25 m) is made of glass to allow visual access. Another wall (i.e., front wall 1 m x 1.5 m) is fitted with a porthole in its center. A square burner (180 mm x 180 mm), with propane (99.5% purity) as fuel, positioned at the center of the enclosure, is used as a fire source in the experiments. The compartment is equipped with supply and extraction lines, positioned at the top of the enclosure. The lines are equipped with sensors to measure the flow characteristics (i.e., flow rate, temperature, pressure) while the species concentrations are measured at the exhaust line only. The extraction line is connected to an exhaust fan equipped with a variable speed drive, while the supply duct is kept open, allowing for fresh air to enter the enclosure (i.e., through natural inflow). The cross-section area for both lines is 60 mm x 60 mm. Due to the length of the ventilation lines (around 20 m, from the fan to the enclosure), pressure drops between the enclosure, and its surroundings are observed. In the range of flow rates studied (i.e., 0 - 50 m³/h), the pressures in the room vary from -700 Pa to 0 Pa, leading to leakage flow rates into the enclosure within the range 0 - 8.4 m³/h. It is worth mentioning that the global equivalence ratio (GER) considered in this study is 0.47 (a thorough discussion on the quantification of the GER is provided in [14]). For more details regarding the experiment, the reader is referred to [15]. Many scenarios have been performed during the campaign and in this study, 6 different cases are selected, as shown in Fig. 1. Five of the cases are in the well-ventilated regime (no extinction), while one case is in the under-ventilated regime (extinction). The nomenclature for the test scenarios is AMXXQYY where ‘XX’ and ‘YY’ represent the fuel flow rate (in g/s) and the extraction flow rate as measured before the fire (in m³/h). It is important to note that, whereas the mass flow rate has been kept constant during the experiments, the volume flow rate increases as the temperature of the extracted hot gases increases. Care must be taken to impose the correct extraction rate in the simulations (i.e., based on the mass flow rate, not on the volumetric flow rate before ignition).

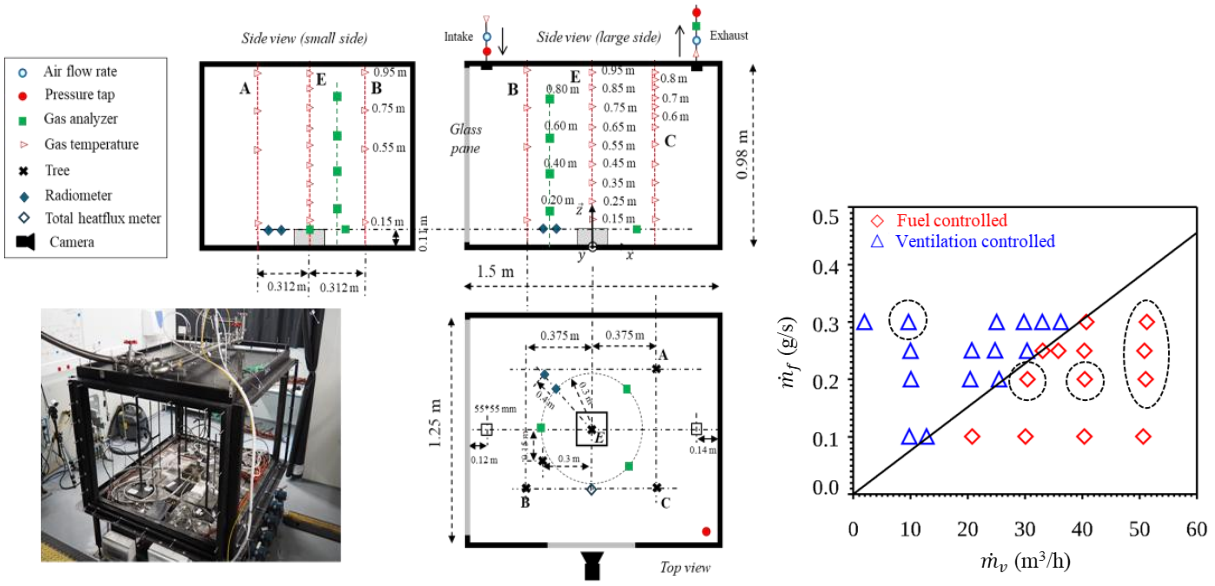


Fig. 1. Illustration of the test case with measurement locations (left) and the selected scenarios for numerical validation (indicated with black circles) (right).

2.2 Modelling and numerical set-up

The LES have been performed using FireFOAM, as available within OpenFOAM v1912 [16], and developed by FM [17]. The Navier-Stokes equations are solved (conservation of mass, momentum, species, and energy). The sub-grid scale turbulence is modelled using the dynamic Smagorinsky model [18] where the turbulence parameters such as c_s, c_l, c_ε, are calculated dynamically in every cell. The turbulent Prandtl number is assumed to be constant (equal to 0.5). All the details are found in [19, 20]. All simulations are performed using the finite-rate chemistry approach with the EDC combustion model using the version that was developed in 2005 [2]. Implementation details are found in [9]. Radiation is modelled using the prescribed radiative fraction approach. The bulk effect of soot in the net emission / absorption has been accounted for through the prescribed radiative fraction as taken from the experiments.

The computational domain is a rectangular box of 1.52 m x 1.22 m x 1 m (length x width x height), shown in Fig. 2. An extension of 0.2 m at the location of the supply and exhaust opening replaces the ductwork. The cross-sections are similar to the experiment. Uniform grid sizes of 3 cm, 2 cm, and 1 cm are used throughout the entire computational domain (including the ducts). The fuel mass flow rates and extraction mass flow rates were set to the corresponding experimental values (i.e., the latter set to the relatively steady values as recorded in the experiments during the fire). The simulations do not consider any leakages. The ambient temperature and pressure were 293 K and 101325 Pa, respectively. The walls surrounding the compartment are assigned to the thermal properties corresponding to the respective materials, and 1D heat transfer is considered. The supply is modelled as 'open', allowing for fresh air to be freely entrained. The boundary condition for velocity at the walls is 'slip' (unless mentioned otherwise) and for species at the same boundaries it is 'zeroGradient'. The simulations for the

non-extinction cases were run for 200 s with a variable time step, based on a maximum CFL number of 0.3. Averaging over a period of 100 s is performed to obtain mean values. The numerical schemes used in the simulations follow the recommendations of [21]. A flame anchoring strategy, prescribing a hot surface temperature for the fuel, is applied. As previously discussed in [9], a value of 900 K is chosen in this study, which is close to the auto-ignition temperature of the fuel. This choice is also supported by the experimentally measured temperatures very close to the burner surface.

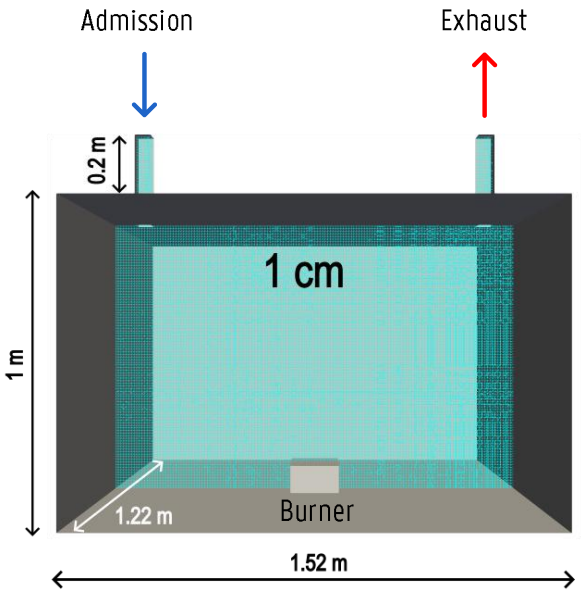


Fig. 2. Illustration showing the computational domain with 1 cm grid size.

2.2 Chemistry mechanisms

Three global propane mechanisms are tested in this study, listed in Table 1.The background discussion regarding the choice of the 2sWD [22] and BE [23] mechanisms is found in [8]. In this work, an additional chemistry mechanism is tested, named 3sFureby[24]: a three-step propane mechanism that includes CO and NO as minor species. It is worth mentioning that this mechanism was validated for high-Reynolds number flames (i.e., a dump combustor) in [24]. Before being validated for LES, the Arrhenius parameters were optimized to match the laminar flame speed and temperature of the GRI3.0 [25] in lean premixed flames. The propane mechanism has been compared with the San Diego mechanisms [26].

The experimental data used in [24] mostly involved counterflow diffusion flame scenarios. Although not developed for fire scenarios, the performance of this mechanism will still be evaluated here, because of the limited availability of reduced (or global) mechanisms. In that sense it is also noted that the global mechanism 2sWD was not developed for fire simulations, either, but it was shown to provide results in reasonable agreement with experimental datafor flame temperature, HRR, and extinction in open atmosphere scenarios in [8, 10].

Table 1. Chemistry mechanisms and their kinetic parameters used in this study.

Mech.	Reactions	Reaction rates [cal/mol, cm, s, mol]
BE [23]	1. $C_3H_8 + 3.5O_2 \rightarrow 3CO + 4H_2O$	$5.82 \times 10^{12} \exp(-34000/RT)[O_2]^{0.86}[C_3H_8]^{0.8}$
	2. $CO + 0.5O_2 \leftrightarrow CO_2$	$2.0 \times 10^{9} \exp(-1200/RT)$
2sWD [22]	1. $C_3H_8 + 3.5O_2 \rightarrow 3CO + 4H_2O$	$1.0 \times 10^{12} \exp(-30000/RT)[C_3H_8]^{0.1}[O_2]^{1.65}$
	2. $CO + 0.5O_2 \leftrightarrow CO_2$	For: $3.98 \times 10^{14} \exp(-40708/RT)[CO]^{1}[O_2]^{0.25}[H_2O]^{0.5}$
		Rev: $5 \times 10^{8} \exp(-40708/RT)\,[CO_2]^{1}$
3sFureby [24]	1. $C_3H_8 + 3.5O_2 \rightarrow 3CO + 4H_2O$	$1.67 \times 10^{17} T^{0.93} \exp(-36942/RT)[C_3H_8]^{0.36}[O_2]^{1.75}$
	2. $CO + 0.5O_2 \leftrightarrow CO_2$	For: $6.61 \times 10^{8} T^{0.87} \exp(-25257/RT)[O_2]^{0.83}$
		Rev: $9.56 \times 10^{7} T^{0.87} \exp(-25257/RT)\,[CO_2]^{0.55}$
	3. $O_2 + N_2 \leftrightarrow 2NO$	$1.5 \times 10^{19} T^{-0.3} \exp(-76388/RT)$

3. Results and discussion

3.1 Well-ventilated conditions

3.1.1 Grid sensitivity analysis

For the grid sensitivity analysis, three well-ventilated scenarios are considered: AM20Q50, AM25Q50, and AM30Q50.

Fig. 3 presents the comparison between the simulations and the experimental measurements for the temperatures above the burner (first row images) and away from the burner (second row images). It is noted that differences between thermocouple temperatures and gas temperatures are small in the present study. Three different grid sizes have been tested, using the 2sWD propane mechanism.

Above the burner, the peak value reported in the experiment is relatively similar in all three cases: around 900 – 1000 K, very close to the burner surface. Above 0.2 m it becomes fairly uniform, between 500 – 600 K. In general, the simulations capture the experimental trends for all three scenarios. Above the burner, the simulations overestimate the peak temperatures , but have very good agreement with the experiments at higher axial locations. Very strictly speaking, no real mesh insensitivity of the results can be claimed and, ideally, 0.5 cm mesh cells should have been tested, but the computational cost was prohibitive. Also, it is natural to observe some mesh sensitivity very close to the burner, given the steep gradients there. It should also be acknowledged that the mesh cell affects the mechanically induced flow field and the near-wall behaviour at the compartment boundaries. The effect thereof is not analyzed in all detail, because the flow field results cannot be validated directly in the absence of experimental data thereof. This is considered future work. Nevertheless, the overall mesh sensitivity of the simulation

results, which are in satisfactory agreement with the experimental data in terms of temperature, is quite small for these EDC simulations with finite-rate chemistry. This provides confidence in their accuracy, so that the analysis on the impact of the finite-rate chemistry mechanism is justified. Among all the tested grid sizes, the results on the 2 cm mesh have the least overestimation (i.e. 15%) of the peak value. While the 3 cm temperature prediction seems very close to the 2 cm results, their predicted HRR is 30% lower than the experiment (which will be discussed later).

Interestingly, the grid dependence of the temperature profiles for this enclosure fire scenario is clearly less prominent compared to open atmosphere scenarios, with the same turbulent combustion models [8, 9]. It is speculated that this is due to the fact that, in contrast to open atmosphere flames, the flow field is now not only determined by the flame itself, but also by the mechanical ventilation and the enclosure geometry. As mentioned, flow field measurements are necessary for more comprehensive validation of the simulation results.

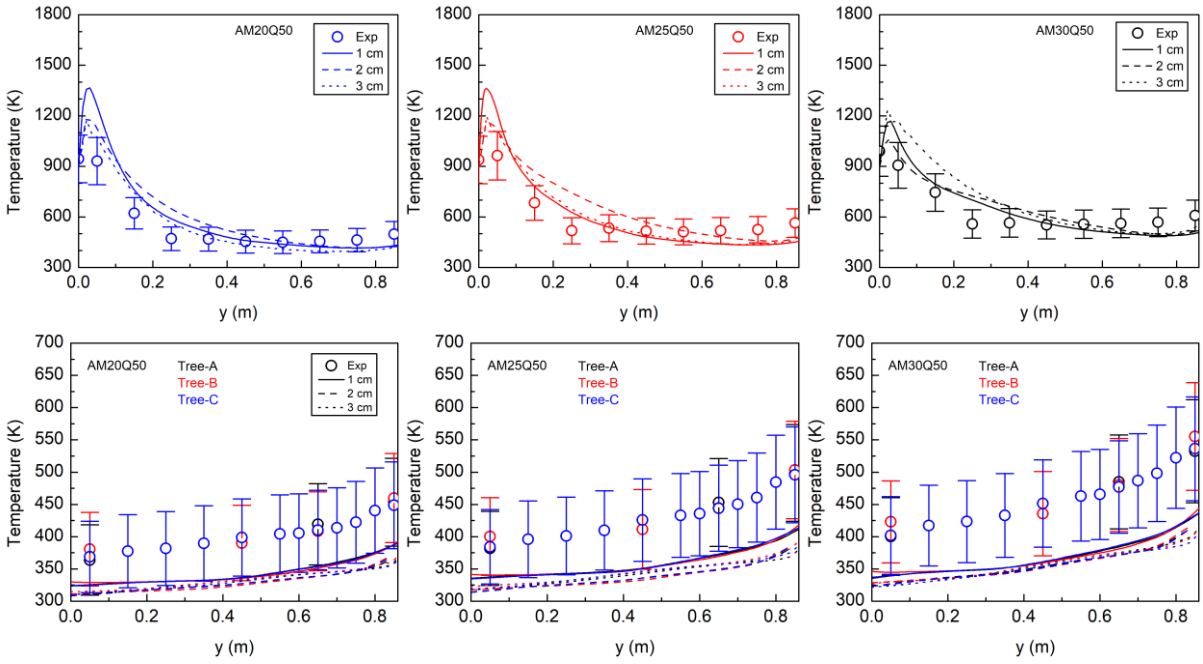


Fig. 3. First row: Temperatures above the burner (tree-E) and second row: away from the burner for three different well-ventilated scenarios.

Away from the burner, the measured temperature values are relatively uniform, both in the experiments and the simulations (second-row images). However, the simulations underpredict the experimental data by about 25% at all heights. This will be discussed later. It is noted that the error bar indicates 10% deviation so that the size of the bar depends on the scaling of the y-axis.

It is recalled that the simulations in this study do not consider leakage. As a result, there is some uncertainty on how the leakage affects locally the flow field and the temperature measurements within the compartment. The leakage flow rate is not necessarily negligible when compared to the mechanically extracted flow rate. A proper validation of the flow field is deemed necessary to assess the aforementioned interactions. Unfortunately, this is not possible in the absence of

detailed experimental data. Hence, this is considered future work, beyond the scope of the present paper.

3.1.2 Heat Release Rate

The comparison of the predicted HRR in the well-ventilated cases is presented in Fig. 4. The HRR in the experiments is post-processed through the carbon dioxide generation (CDG) method, using the measured concentrations of CO and CO_2 in the exhaust duct [27]. The peak at the beginning of the experiment is due to the sudden increase of combustion products when the flame was ignited. The HRR becomes more or less constant when the flame is stabilized. In the simulations, this phenomenon is not observed. It is because the flame was ignited immediately in the simulations, whereas in the experiment, some gaseous fuel could pile up in the enclosure during the short period between the opening of the gas valve and the actual ignition of the flame

The values in Table 2 show that the largest discrepancy between the HRR obtained in the simulations and the HRR as calculated from the fuel mass flow rate imposed in the experiments (assuming complete combustion) is around 30%, on the 3 cm grid size. The 1 cm mesh almost fully recovers the HRR from the experiment. The 2 cm grid results recover around 90% of the experimentally imposed HRR. Therefore, and given the discussion in Section 3.1.1, the remainder of the analysis is performed on results on the 2 cm mesh.

At this point, it is interesting to evaluate the HRR with the three different global mechanisms (i.e., 2sWD, BE, and 3sFureby), as presented in Fig. 4. The 2sWD and BE mechanisms recover the experimental value fairly well, while the 3sFureby underestimates the experimental HRR by 30% (i.e., only around 10 kW out of the expected 14 kW). The distribution of the fuel (i.e. C_3H_8) mass fraction inside the compartment, shown in Fig. 5 (contour plot), reveals the reason: more fuel escapes from the domain with the 3sFureby mechanism. The contour plots differ massively from the ones with 2sWD.

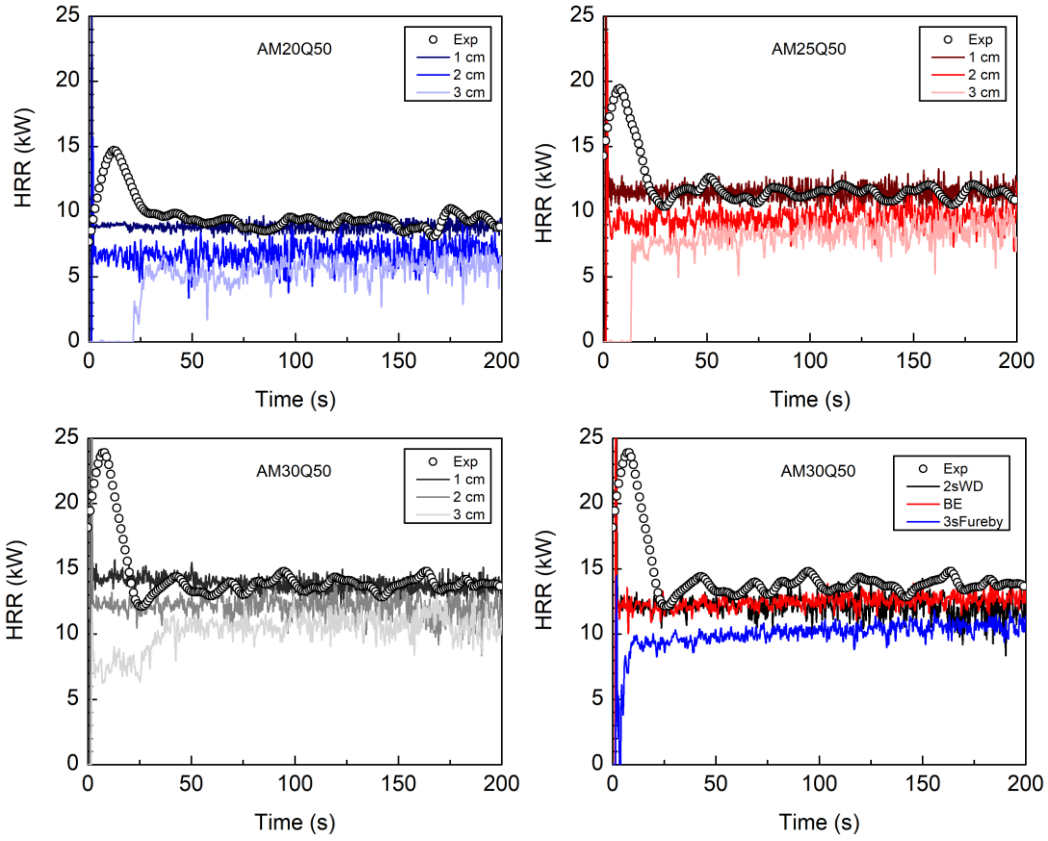


Fig. 4. Heat release rate prediction from the simulations for various grid sizes and mechanisms, compared to the post-processed values from the experiments. Top figures and bottom left figure: results with 2sWD. Bottom right figure: 2 cm mesh results.

Table 2. HRR (kW) comparison between simulations and experiments.

Case	**3 cm**	**2 cm**	**1 cm**	**Exp**
AM30Q50	10.5	12.5	14.0	14.1
AM25Q50	8.7	10.0	11.5	11.6
AM20Q50	6.0	7.5	8.9	9.1

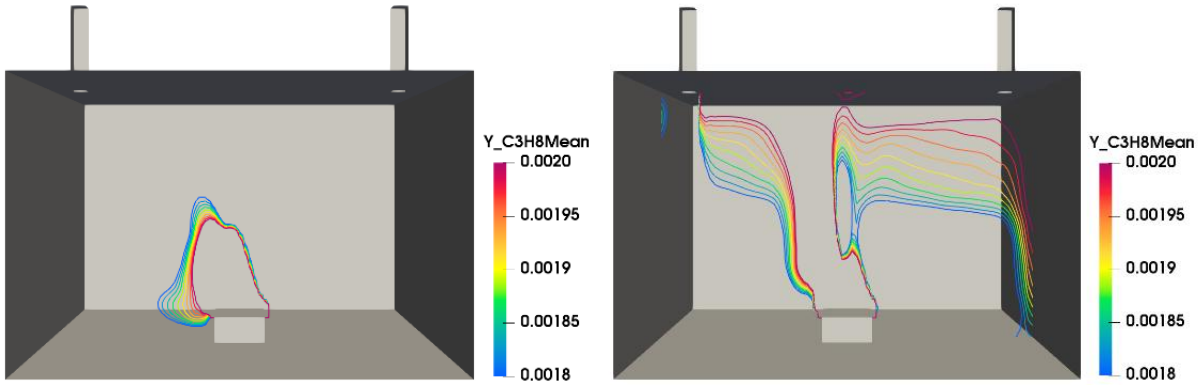


Fig. 5. Contour plot of mean C_3H_8 mass fraction dispersion inside the enclosure in the AM30Q50 scenario with 2sWD (left) and 3sFureby (right).

3.1.3 Temperature

The focus of this section revolves around the effect of the different reaction mechanisms, the fuel mass flow rate, and the exhaust flow rate. Similarly to section 3.1.1 Grid sensitivity analysis this section analyses the temperature predictions above the burner (thermocouple Tree E) and away from the burner. For the latter, only thermocouple tree C is considered, as the temperature field is quite uniform (see Fig. 3).

Fig. 6 presents 2D plots of the mean temperature fields for the three different reaction mechanisms. Qualitatively, the 2sWD shows the lowest temperature inside the flame zone (i.e., above the burner surface), predicting a maximum temperature of about 1300 K. The BE results reveal the largest hot zone (indicated by the red hue). Although the highest temperature with BE and 3sFureby is up to 500 K higher temperature than with 2sWD, all plume shapes are comparable, with some flame tilting towards the air supply side.

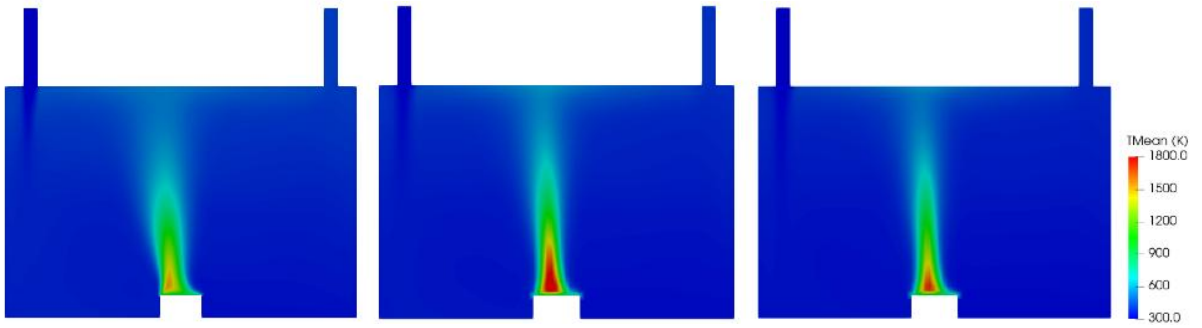


Fig. 6. Simulation results for the AM30Q50 scenario showing the mean temperature field for three different mechanisms: 2sWD (left), BE (middle), and 3sFureby (right).

Fig. 7 presents a quantitative comparison. Very significant differences are observed above the burner. The 2sWD mechanism predicts temperatures that are within 10% of the experimental values near the burner surface. Despite the overestimation in the zone 0.2 – 0.35 m above the burner, the prediction again improves higher up, maintaining almost 90% accuracy compared to the experimental values. The BE and 3sFureby perform similarly to the 2sWD in the latter region

(i.e., 0.45 – 0.8 m above the burner), but the temperature predictions near the burner surface are off by more than 70 %. Away from the burner, the differences between the simulation results are much smaller, all of them under-predicting the experimental data, while capturing the trend. Based on these results, the 2sWD is considered the most suitable mechanism for the scenario at hand.

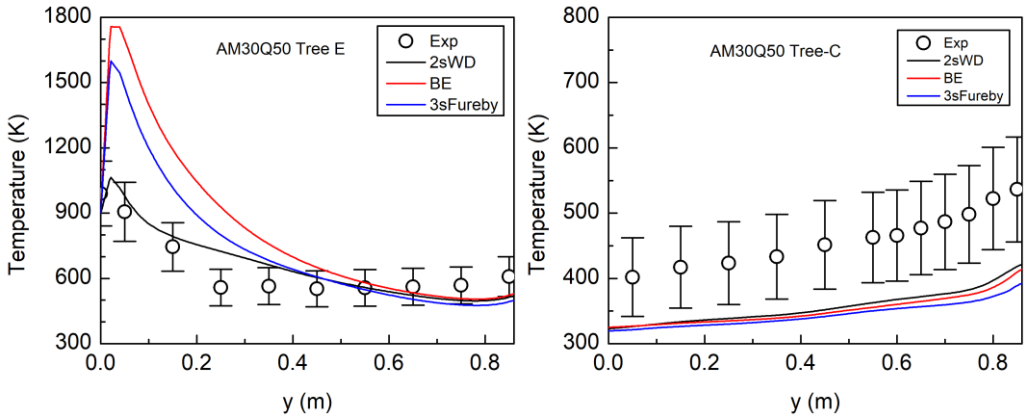


Fig. 7. Temperature predictions in the AM30Q50 scenario with various mechanisms. Left: measurements above the burner surface (thermocouple tree E). Right: measurements away from the burner (thermocouple tree C). Grid size: 2 cm.

The strong deviations from the experimental data with the BE and 3sFureby mechanisms, might be due to the fact that they were not calibrated for flames with low levels of turbulence intensity. The BE mechanism was calibrated for piston (engine) combustion applications and was validated for pressures of 6 – 20 bar. These conditions are totally different from the ones encountered in fire scenarios. In our previous work, in open-atmosphere propane flames [8], the temperature predictions did not deviate as significantly from the ones obtained with 2sWD. However, in the present study there is far more complex interaction between the flames and the flow field, the latter being largely affected by the enclosure geometry and mechanically imposed flow rate. The results clearly reveal how sensitive the global mechanism is, and that validation for a certain configuration is no guarantee for accuracy and reliability in other scenarios. The 3sFureby mechanism was derived from the GRI3.0 mechanism for lean premixed C_3H_8 – air flames. The mechanism was validated in [24] for LES simulations of turbulent combustion with high Reynolds (and moderate Damköhler number). This is again far from the conditions in the study at hand. As it stands, the applicability of these global mechanisms seems limited in fire scenarios, and certainly strongly scenario dependent. It is noted that, despite the good agreement for the 2sWD mechanism (which was not developed for low turbulence intensity flames, either) here, as well as in the free burn scenarios in [8], this is no guarantee for general reliability and accuracy in any fire scenario yet.

The second analysis focuses on the effect of fuel mass flow rate and ventilation flow rate. The contour plots of Fig. 8 show the mean temperature field for fixed fuel mass flow rate and three extraction flow rates (AM20Q50, AM20Q40 and AM20Q30). Increasing the extraction rate,

while keeping the fuel mass flow rate fixed, leads to reduced flame heights (AM20Q30 > AM20Q40 > AM20Q50) and reduced maximum temperatures. This is presumably due to the extraction of more heat per unit time from the enclosure, as well as some cooling of the flame by excess air (as supplied by the mechanical ventilation) and potentially by the increased leakage flow rate. Although not very outspoken, there is also somewhat less tilting towards the air-supply duct as the extraction flow rate is reduced.

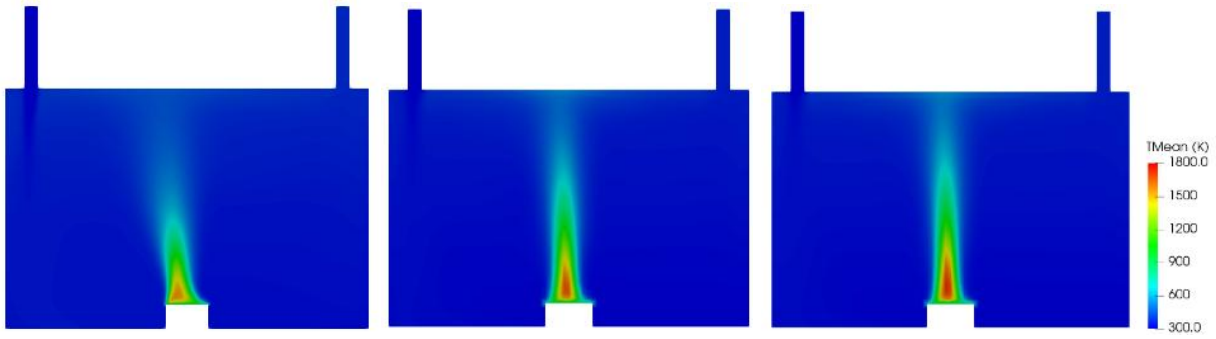


Fig. 8. Predicted mean temperature field for AM20Q50 (left), AM20Q40 (middle), and AM20Q30 (right). Performed with the 2sWD mechanism on the 2 cm mesh.

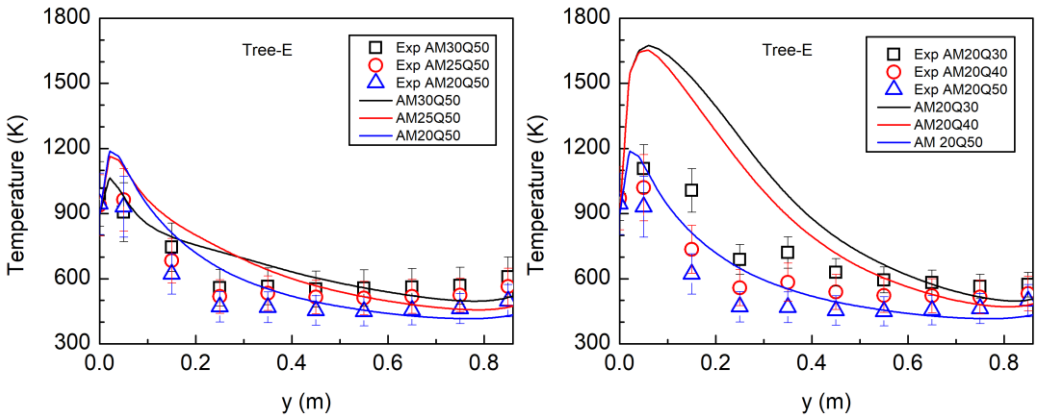


Fig. 9. Temperature predictions of 3 well-ventilated scenarios with varying fuel flow rate (left); AM30Q50, AM25Q50, AM20Q50 and varying ventilation flow rate (right); AM20Q30, AM20Q40, AM20Q50. Performed with the 2sWD mechanism on the 2 cm mesh.

Interestingly, the impact of the ventilation flow rate on the temperatures above the burner is much stronger than that of the fuel mass flow rate (Fig. 9). Whereas this qualitative observation is confirmed in the simulations, the differences between the simulations and the experiments become very large at reduced extraction flow rate. This is a clear indication of the importance of the flow field, as discussed in the next section.

3.1.4 Flow field

As mentioned, the flow field inside the enclosure in a mechanically ventilated scenario results not only from the buoyancy as generated by the flame, but also from the flow as generated by the mechanical ventilation system. Unfortunately, no flow field measurements are available. Still, an analysis, solely focusing on the simulations, is presented.

The predicted air supply flow rates are listed in Table 3. The experimental value was measured at the air supply line, computed from the pressure difference recorded by bidirectional Pitot probe. In the simulation, it was calculated from the integration of the vertical velocity component over the area of the supply duct. Overall, the simulations over-predict the air supply through the duct, by less than 10%. Again, the absence of leakage in the simulations may partly explain the discrepancy.

However, there is a very strong effect of the boundary conditions. This is demonstrated in Fig. 10, comparing results for AM30Q50 and AM25Q50 when applying 'no slip' and 'slip' BC for the velocity at the walls

On a 2 cm mesh it is not possible to accurately resolve the flow field inside the ducts, nor the flow close to any of the solid boundaries of the compartment. Therefore, it is interesting to explore the near-wall treatment in the simulations. An extensive in-depth analysis is considered future work, but in the present study the 'no slip' BC is explored. Fig. 10 reveals that with this BC there is hardly any flame tilting, and the flames are much higher. As mentioned before, direct validation of flow fields is not possible in the absence of experimental data, but as flame tilting was observed experimentally, and the flame tip appears in better agreement with the experiments (not shown), it is argued that with the present settings and the configuration at hand, the slip BC seems to be the better choice here. This is confirmed in Fig. 11, showing the temperature profiles, when considering the results above the burner. However, away from the burner (thermocouple tree C), the results with no slip BC are closer to the experimental data. Overall, this underscores the need for more detailed flow field information for a more direct and more complete validation of the simulation results.

Table 3. Comparison of the predicted air supply flow rates for each scenario considered.

Case	**Exp. Air Supply (m^3/h)**	**Exp. Leakage (m^3/h)**	**Predicted Air Supply (m^3/h)**		
			3 cm	**2 cm**	**1 cm**
AM30Q50	38	8	41.1	42.3	42
AM30Q50 (BE)			-	41.5	-
AM30Q50 (3sFureby)			-	41.5	-
AM25Q50	38	8.5	41.6	42.6	42.6
AM20Q50	40	9	43.8	44.8	44.3
AM20Q40	31	5.5	-	34.3	-
AM20Q30	24	3.5	-	24.8	-

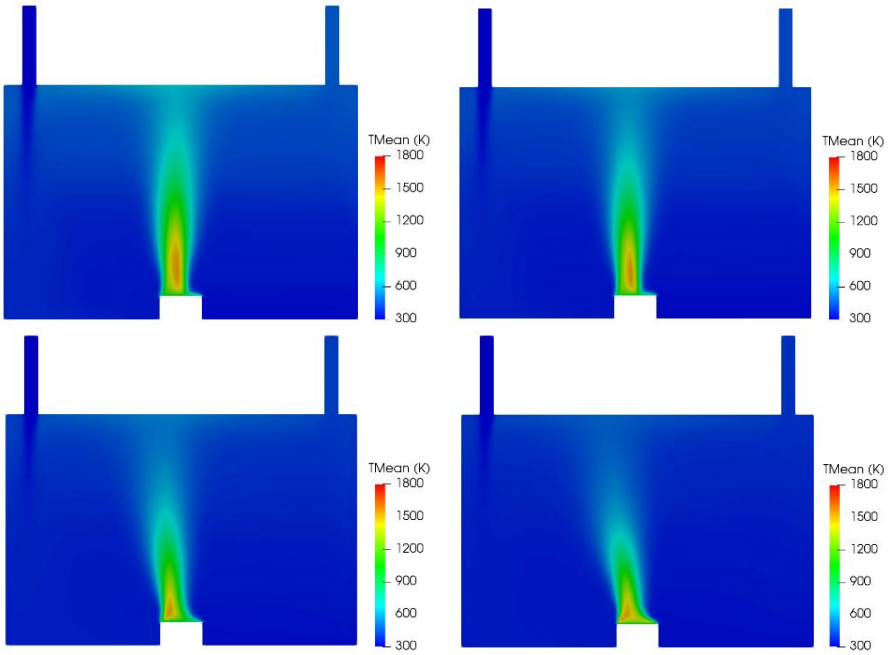


Fig. 10. Predicted mean temperature field for AM30Q50 (left-column) and AM25Q50 (right-column) scenarios with two different boundary conditions for velocity at the walls: no slip (top-row) and slip (bottom-row).

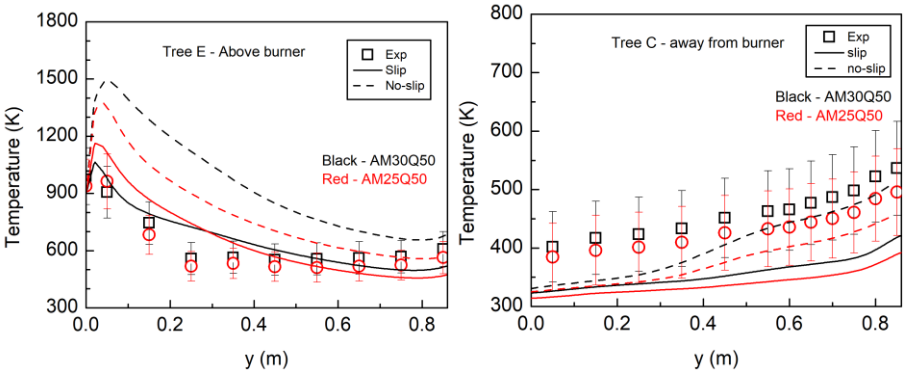


Fig. 11. Quantitative comparison of temperature predictions between cases with slip (dashed lines) and non-slip (solid lines) BC for velocity at the walls.

3.2 Under-ventilated conditions

The selected scenario is AM30Q10, which had the highest fuel mass flow rate ($\dot{m}_{C_3H_8}$= 0.3 g/s) and the lowest extraction flow rate ($\dot{V}_{ext}$ before fire = 10 m³/h). This case therefore experienced the shortest time to total extinction in the experiments. Hence, this case was selected to reduce computational costs. As part of the safety precautions within the facility, the fuel flow rate was immediately shut once the flame disappeared inside the compartment, so that ignition of unburnt fuel after extinction could not take place.

Fig. 12 presents the HRR results. The experimental HRR values stabilize around 13 kW after 20 s. After about 140 s, the HRR starts to decrease, with total extinction after 160 s. The HRR as predicted with the 2sWD and BE closely follows the experimental trend up to 100 s. The 2sWD results predict a gradual decrease in HRR after 200 s (i.e., with a 60 s delay compared to the experiments), whereas the BE still continues to maintain the peak HRR up until 360 s (i.e., with 220 s delay). The fact that BE reaches extinction at a later stage (i.e., only at a very low oxygen concentration limit) is in line with what has been reported in [10]. Interestingly, significant fluctuations (or oscillatory behaviour) are observed in the HRR plots in all the simulations after the initial HRR decay. These fluctuations are due to ignition of unburnt fuel that is constantly injected into the compartment. The anchoring strategy in the simulations (i.e., imposing a temperature of 900 K just above the burner) provides a sufficient amount of energy to ignite the unburnt fuel inside the compartment. Whether or not this phenomenon is realistic cannot be validated with the current experiments, because, as mentioned, the fuel flow rate was manually closed for safety reasons in case of total extinction. It is considered interesting to further evaluate the finite-rate chemistry approach (using the selected mechanisms) in the context of this re-ignition phenomenon. It shows the potential of the approach to predict ignition and oscillatory behavior of the flame in under-ventilated compartment fire scenarios.

Finally, it is noted that the 3sFureby experienced a similar fluctuation and the gradual decrease in HRR also occurred at about the same time as with the 2sWD, but similarly to what was observed in the well-ventilated scenario, it under-predicted the experimental HRR by about 25%.

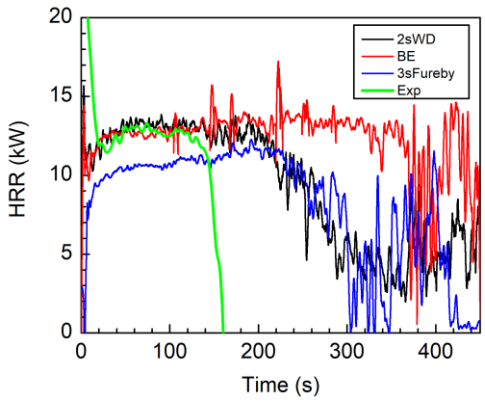


Fig. 12. Comparison of the estimated HRR from the simulations (using a 2 cm grid size) and experiment for AM30Q10 case, with various chemistry mechanisms.

4. Conclusions

LES of mechanically ventilated enclosure fires were performed using the EDC approach with finite-rate chemistry, in five well-ventilated and one under-ventilated experimental scenarios.

Mesh sensitivity studies showed that temperature predictions were relatively less sensitive to grid size compared to open atmosphere flames, simulated with the same settings, in previous work [8, 9]. One possible reason is the strong influence of mechanical ventilation on the flow field. Taking into account temperature predictions (above the burner surface and away from the burner), as well as HRR predictions, a 2 cm cell size was chocen as the baseline grid resolution.

The simulation results revealed only a moderate impact of the fuel flow rate (i.e., AM20Q50 – AM30Q50) on the temperature. The effect of extraction flow rate (AM20Q30 – AM20Q50), on the other hand, was strong, particularly above the burner. Whereas agreement with experimental data was reasonable for the scenarios with the highest extraction rate (less than 10% deviation), the temperatures were significantly overpredicted above the burner for lower extraction rates (up to 60% deviation). Detailed flow field measurements should allow for a more in-depth study on these deviations. This is considered future work.

Among the chemistry mechanisms tested, the 2sWD mechanism provided the best overall agreement with experiments for both temperature and HRR. The BE and 3sFureby mechanisms showed substantial temperature overprediction and, in the case of 3sFureby, significant HRR underprediction. The latter is caused by the unburnt fuel escaping from the computational domain. This confirms that validation of reduced chemistry models, not developed specifically for fire flame situations, is strongly scenario dependent and hence cannot be readily generalized.

The wall boundary condition was also shown to be very important. With the given mesh resolution, slip wall conditions yielded better agreement for temperatures above the burner, as well as for flame tilting, whereas no-slip conditions led to better agreement of the temperature results with experimental data away from the burner. More direct and complete validation requires detailed information about the flow field, which is not available.

The simulations also compared the 3 different chemistry mechanisms for an under-ventilated scenario (i.e., AM30Q10), which led to total extinction during the experiment. The gradual decrease of HRR was confirmed in the simulations, albeit with some delay (of around 60 s with 2sWD and 3sFureby, and around 220 s with BE). The 3sFureby underestimated the HRR before extinction, similarly to the well-ventilated scenarios. In general, although the extinction was delayed and less sudden when compared to the experiments, the 2sWD showed again the best agreement. All simulations predicted re-ignition of unburnt fuel immediately after extinction, leading to oscillations in HRR. This could not be validated, as the fuel supply was shut down immediately after extinction in the experiments, for safety reasons.

In general, the paper highlighted the potential impact of the flow field within the compartment, in combination with the flame dynamics (which is governed by mixing and chemistry). The quantification of the flow field should be considered in future research.

Acknowledgements

This research is funded by The Research Foundation-Flanders (FWO-Vlaanderen) via PhD fellowship 1104125N and projects G023221N and G034725N, and by the OFFERR project for the European user facility network.

Author contributions

Jeri At Thabari, Conceptualization; investigation, Performing simulations; Formal analysis; Writing original Draft. **Georgios Maragkos**, Conceptualization; supervision, review & editing. **Youk Moorthamers**, Conceptualization; review & editing. **Alexander Y. Snegirev**,

Conceptualization; review & editing. **Hugues Pretrel**, Investigation, experimental data curation, review & editing. **Bart Merci**, Conceptualization; Supervision, writing, project administration, funding acquisition, review & editing.

References

[1] D.B. Spalding, Mixing and chemical reaction in steady confined turbulent flames, Symposium (International) on Combustion, 1971;13: 649-57. https://doi.org/10.1016/S0082-0784(71)80067-X

[2] B.F. Magnussen. The eddy dissipation concept: A bridge between science and technology. ECCOMAS thematic conference on computational combustion, 2005, p. 24.

[3] G. Maragkos, T. Beji, B. Merci, Advances in modelling in CFD simulations of turbulent gaseous pool fires, Combustion and Flame, 2017;181: 22-38. https://doi.org/10.1016/j.combustflame.2017.03.012

[4] L. Jiang, A.S. Bøe, T. Li, Numerical simulation of fire spread in a large-scale open CLT compartment, Fire Safety Journal, 2024;150: 104289. https://doi.org/10.1016/j.firesaf.2024.104289

[5] J.P. White, S. Vilfayeau, A.W. Marshall, A. Trouvé, R.J. McDermott, Modeling flame extinction and reignition in large eddy simulations with fast chemistry, Fire Safety Journal, 2017;90: 72-85. https://doi.org/10.1016/j.firesaf.2017.04.023

[6] A.Y. Snegirev, Perfectly stirred reactor model to evaluate extinction of diffusion flame, Combustion and Flame, 2015;162: 3622-31.

[7] B. Magnussen. On the structure of turbulence and a generalized eddy dissipation concept for chemical reaction in turbulent flow. 19th aerospace sciences meeting, 1981, p. 42.

[8] J. At Thabari, G. Maragkos, Y. Moorthamers, A. Snegirev, B. Merci, Numerical study of the impact of global mechanisms in LES of propane pool fire using the EDC - finite-rate chemistry approach, Fire Safety Journal, 2025;156: 104472. https://doi.org/10.1016/j.firesaf.2025.104472

[9] J. At Thabari, G. Maragkos, A. Snegirev, B. Merci, Numerical study of the impact of the EDC formulation and finite-rate chemistry mechanisms in CFD simulations of fire plumes, Fire Safety Journal, 2023;141: 103950. https://doi.org/10.1016/j.firesaf.2023.103950

[10] J.A. Thabari, B. Kruljevic, G. Maragkos, A. Snegirev, B. Merci, Assessment of the EDC/finite rate chemistry approach towards predicting extinction in a turbulent buoyant diffusion flame, Proceedings of the Combustion Institute, 2024;40: 105602.

[11] D. Myilsamy, C.B. Oh, J. Jeon, Large eddy simulations of pool fires and backdraft in a compartment using FDS and FireFOAM, Case Studies in Thermal Engineering, 2025;72: 106337. https://doi.org/10.1016/j.csite.2025.106337

[12] H. Prétrel, N. Chaaraoui, B. Lafdal, S. Suard, Effect of environmental conditions on fire combustion regimes in mechanically-ventilated compartments, Fire Safety Journal, 2022;127: 103493. https://doi.org/10.1016/j.firesaf.2021.103493

[13] H. Prétrel, L. Bouaza, S. Suard, Multi-scale analysis of the under-ventilated combustion regime for the case of a fire event in a confined and mechanically ventilated compartment, Fire Safety Journal, 2021;120: 103069. https://doi.org/10.1016/j.firesaf.2020.103069

[14] H. Pretrel, J.A. Thabari, G. Maragkos, Y. Moorthamers, A. Snegirev, B. Merci, The importance of the GER definition in the analysis of combustion regimes in a closed mechanically ventilated compartment, Journal of Physics: Conference Series, 2025;3121: 012015. 10.1088/1742-6596/3121/1/012015

[15] H. Pretrel, J. At Thabari, G. Maragkos, Y. Moorthamers, A.Y. Snegirev, B. Merci, New insights into fire combustion regimes in a closed mechanically ventilated compartment through experimental and theoretical analysis, Fire Safety Journal, 2025;Submitted for publication.

[16] OpenCFD, OpenCFD Release OpenFOAM® v1912. https://www.openfoam.com/news/main-news/openfoam-v1912, 2019 (Accessed 02 February 2023)

[17] A. Krisman, X. Lu, D. Mohaddes, N. Ren, Y. Wang, FM's public-facing FireFOAM release. https://github.com/fmglobal/fireFoam, 2025 (Accessed 14 September 2025)

[18] P. Moin, K. Squires, W. Cabot, S. Lee, A dynamic subgrid-scale model for compressible turbulence and scalar transport, Physics of Fluids A: Fluid Dynamics, 1991;3: 2746-57.

[19] G. Maragkos, B. Merci, On the use of dynamic turbulence modelling in fire applications, Combustion and Flame, 2020;216: 9-23. https://doi.org/10.1016/j.combustflame.2020.02.012

[20] G. Maragkos, A.Y. Snegirev, J. Thabari, B. Merci. Flame ignition and extinction modelling using infinitely fast chemistry in large eddy simulations of fire-related reacting flows. 14th International Symposium on Fire Safety Science, 2023, Tsukuba.

[21] G. Maragkos, S. Verma, A. Trouvé, B. Merci, Evaluation of OpenFOAM's discretization schemes used for the convective terms in the context of fire simulations, Computers & Fluids, 2022;232: 105208. https://doi.org/10.1016/j.compfluid.2021.105208

[22] C.K. Westbrook, F.L. Dryer, Simplified reaction mechanisms for the oxidation of hydrocarbon fuels in flames, Combustion Science and Technology, 1981;27: 31-43.

[23] CERFACS. CERFACS chemistry mechanisms lists. In. CERFACS chemistry mechanisms lists.

[24] V. Sabelnikov, C. Fureby, LES combustion modeling for high Re flames using a multi-phase analogy, Combustion and Flame, 2013;160: 83-96. https://doi.org/10.1016/j.combustflame.2012.09.008

[25] G.P. Smith, D.M. Golden, M. Frenklach, N.W. Moriarty, B. Eiteneer, M. Goldenberg, C.T. Bowman, R.K. Hanson, S. Song, J. W.C. Gardiner, V.V. Lissianski, Z. Qin, GRI-Mech 3.0. http://www.me.berkeley.edu/gri_mech/, (Accessed 05 September 2025)

[26] J.C. Prince, C. Treviño, F.A. Williams, A reduced reaction mechanism for the combustion of n-butane, Combustion and Flame, 2017;175: 27-33. https://doi.org/10.1016/j.combustflame.2016.06.033

[27] H. Pretrel, W. Le Saux, L. Audouin, Experimental determination of fire heat release rate with OC and CDG calorimetry for ventilated compartments fire scenario, Fire and Materials, 2014;38: 474-506. https://doi.org/10.1002/fam.2193